

Enhanced Fluorescence, Raman Scattering, and Higher Order Raman Modes in ZnO:Ag Nanorods

R. Udayabhaskar · R. V. Mangalaraja · B. Karthikeyan

Received: 17 September 2014 / Accepted: 4 January 2015 / Published online: 4 March 2015
© Springer Science+Business Media New York 2015

Abstract We report exciton and phonon properties of pure and Ag-modified ZnO nanostructures are prepared using solution-based refluxing route. X-ray diffraction studies show lower angle shift in the characteristic diffraction peaks of ZnO. Additional diffraction peaks related to nano-sized Ag were observed from XRD. Broad absorption band (which covers the 400–1000 nm range) results from surface plasmon resonance (SPR) absorption of metallic silver is observed from optical absorption studies. Enhancement in luminescence and Raman scattering is observed in Ag-modified sample when compared with pure ZnO sample. This is attributed to the presence of metallic Ag in the samples, and we attempted to understand the observed enhancement from the perspective of the local field associated with the metal nanoparticles.

Keywords Metal nanoparticle · Local field · Enhanced photoluminescence · Enhanced Raman scattering · Metaloxide:metal

Electronic supplementary material The online version of this article (doi:10.1007/s11468-015-9877-6) contains supplementary material, which is available to authorized users.

R. Udayabhaskar · B. Karthikeyan (✉)
Department of Physics, National Institute of Technology,
Tiruchirappalli 620 015, India
e-mail: uday.rednam@gmail.com

B. Karthikeyan
e-mail: balkarin@yahoo.com

R. V. Mangalaraja
Department of Materials Engineering, University of Concepcion,
Concepcion, Chile

Introduction

Biological applications such as imaging, sensing, etc. can be addressed by the use of hybrid nanocomposites formed by metal-oxide:metal systems [1–4]. ZnO as a capping layer along with other semiconductor quantum dots (QD) was used to form heterojunction (core/shell) nanocrystals to enhance the photostability of QD's and was successfully used as fluorescence probes for bio-labeling/imaging [5, 6]. Surface-modified ZnO nanoparticles served as potential candidates in medicinal applications [7]. This surface modification may affect the emission properties ZnO nanostructures. Hybrid metal-oxide:metal nanocomposites can overcome this by the presence of metal nanoparticles in the nanocomposites. Thus, the requirements of the technological applications can be met by designing hetero-ZnO/metal nanostructures with multiple/novel properties. Among metal nanoparticles, noble metal nanoparticles showing surface plasmon resonance (SPR) associated with collective oscillation of conduction electrons exhibit absorption in the visible range. Noble metal nanoparticles are promised candidates for metal nanoparticle induced surface-enhanced Raman scattering (SERS) and surface-enhanced fluorescence (SEF) or metal-enhanced fluorescence (MEF) mechanisms for rapid detection of trace level impurities/bio-imaging applications [8–13]. Optical absorption spectra of noble metal nanoparticles such as Ag and Au exhibit strong SPR-related band at ~430 and ~530 nm, respectively. The optical and electrical properties of these metal nanoparticles are influenced by nanoparticles size, shape, and surrounding medium. Presence of metal nanoparticles leads to enhanced-Raman scattering and exhibits enhancement/quenching in fluorescence of the nearby fluorophores or surrounding medium. Local field enhancement in the vicinity of metal nanoparticles and electrons transfer between the metal and metal oxide system plays a key role in deciding the use of these heterosystems for SERS and SEF applications [14, 15].

In this letter, we report synthesis of pure and Ag-modified ZnO nanorods. The synthesis method used is simple in preparation, cheap in cost, and less toxic to improve the luminescence and Raman scattering of ZnO. Our experimental result shows an improvement/enhancement in luminescence and Raman scattering after Ag modification. Possible reasons for the observed enhancement in luminescence and Raman scattering in Ag-modified ZnO nanorods when compared with pure ZnO nanorods are discussed. Here, we demonstrate remarkable optical effects, which stems from collective interactions of metal nanoparticles and metal oxide nanorods.

Experimental

High-purity chemicals zinc nitrate, silver nitrate, and hexamethylenetetramine (HMTA) are used for synthesis of pure ZnO and Ag-modified ZnO nanostructures. The synthesis of the nanorods is as follows: pure ZnO nanorod (without silver content) sample was prepared by mixing clear solutions of 100 ml (0.1 M) zinc nitrate and 100 ml (0.1 M) hexamethylenetetramine (using double-distilled (DD) water), and the resulting solution is refluxed for ~8 h. In the same manner, Ag-modified ZnO nanostructures are prepared by using 0.001, 0.003, and 0.005 M solutions of silver nitrate along with 0.099, 0.097, and 0.095 M zinc nitrate solutions, respectively. The final solutions after the addition of 100 ml (0.1 M) HMTA were refluxed for ~8 h. The precipitates collected with prior washing and dried in a hot air oven at ~60 °C for about ~4 h. Here, after the samples are represented by the code name as ZAg0, ZAg1, ZAg3, and ZAg5 based on the Ag content used in the synthetic process (i.e., 0.0, 0.001, 0.003, and 0.005 M Ag precursor, respectively). The crystalline structure of the prepared samples was investigated with *Rigaku Dmax 2000* X-ray diffraction (XRD) instrument in 20–80° diffraction angle range (2θ). For optical characterizations, 3 mg of prepared sample mixed with 5 ml of DDW and sonicated for 15 min is used for UV–Visible absorption and photoluminescence (PL) studies. Optical absorption spectra of the samples were recorded using *Lamda35* dual beam spectrometer in the range of 300–1000 nm. *HORIBA JobinYvon (Fluoromax)* fluorometer with an excitation wavelength of 330 nm is used for PL measurements. Raman scattering measurements were recorded using *RENISHAW inVia Raman Microscope* with an excitation source of Ar ion laser having wavelength of 514.5 nm.

Results and Discussions

The powder X-ray diffraction patterns of the prepared unmodified and silver-modified ZnO samples were shown in Fig. 1. The diffraction patterns of unmodified ZnO sample (ZAg0) indexed with the hexagonal wurtzite

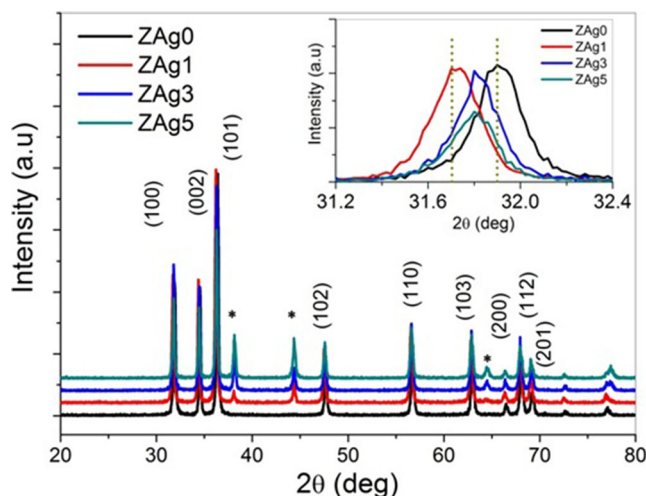
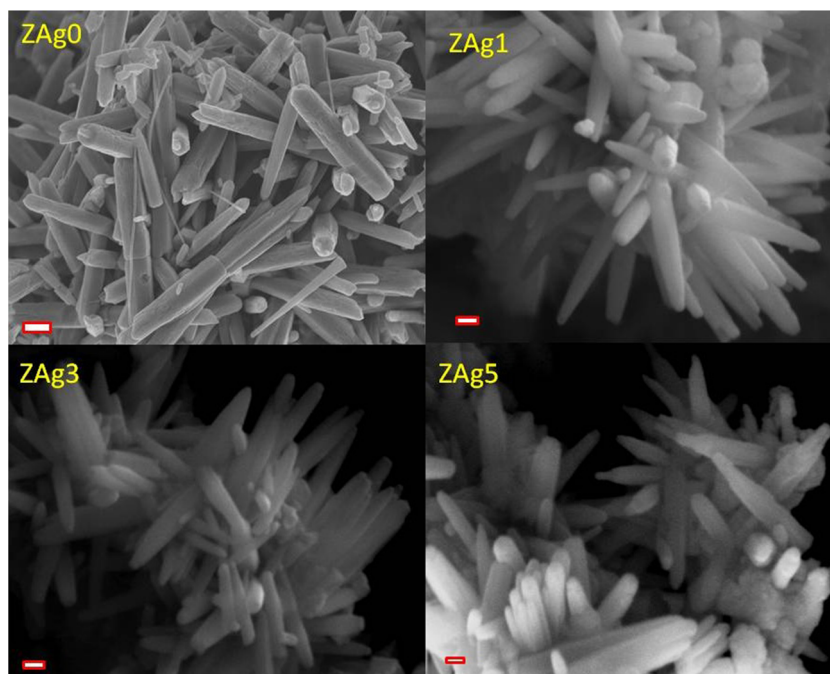


Fig. 1 XRD patterns of the pure ZnO and ZnO:Ag nanostructures

structure of ZnO. The strongest peaks located at 31.91°, 34.56°, and 36.39° correspond to (100), (002), and (101) diffraction planes of hexagonal wurtzite ZnO, respectively. The other peaks representing the (102), (110), (103), (200), (112), and (201) planes of hexagonal wurtzite ZnO are also indexed in the XRD pattern [13]. The diffraction patterns obtained from Ag-modified ZnO samples (ZAg1, ZAg3, and ZAg5) shows the typical diffraction pattern of hexagonal wurtzite ZnO. From the diffraction patterns of the Ag-modified sample characteristic peaks (marked with “*”) of metallic Ag are identified (JCPDS, #893722). The presence of silver during synthesis may results in the substitution of Ag into the ZnO lattice at Zn site and also leads to segregation of silver. The lower angle shift observed from the XRD patterns (inset of Fig. 1) is due to substitution of lower ionic radius Zn^{2+} ions (74 pm) with higher ionic radius Ag^+ ions (122 pm). The observed extra peaks related to metallic silver (whose intensity increases with increase in Ag content) supports segregation of Ag as particles. Further decrease in the intensity of diffractions peaks of ZnO is observed with the increase in Ag content used during synthesis [16, 17]. Scanning electron microscopy images (provided as Fig. 2) depict a rod-like morphology of the prepared samples. The TEM images of the prepared Ag-modified samples shown in Fig. 3 depict rod-like morphological features of ZnO and also showing nearly spherical Ag NPs over them. Electron dispersive X-ray spectroscopy analysis (EDX) of ZAg3 and ZAg5 samples is carried out and the results are provided as [Supplementary material](#). From the FESEM image of ZAg5 ([Supplementary material](#)) it is observed rod-like morphological features and also nearly spherical particles. The extra diffraction peaks related to metallic Ag observed in XRD and EDX analysis supports the presence of the Ag particles in the samples.

Fig. 2 Scanning electron microscope (SEM) images of the Ag-modified ZnO samples. Scale bar for all the images is 200 nm



Optical Studies

Optical absorption spectra of the pure and Ag-modified ZnO nanorods are shown in Fig. 4a. The absorption peak that corresponds to excitonic absorption of ZnO appeared at around 368 nm for pure ZnO nanorods. This peak shows redshift in the Ag-modified samples, and this shift is independent of Ag content used during synthesis. An intense absorption feature is observed which nearly covered the visible region, and near NIR (400–1000 nm) arises from the surface plasmon resonance (SPR) absorption of Ag nanoparticles whose presence along with ZnO is supported by the XRD studies. The shift and shape variations observed in the plasmon band of Ag in the absorption spectra are due to the influence of shape changes (variation from the spherical shape) and dielectric constant of the surrounding medium. Metal nanoparticle with non-spherical nature usually shows

broad/multiple bands in their optical absorption spectrum [18]. A redshift, indicative of band gap decrease is reported earlier for ZnO by doping [19–21]. The shift in the excitonic absorption band and observation of distinctly broad absorption band in the visible range is due to doping of Ag and presence of Ag nanoparticles with a strong interfacial coupling/interaction with ZnO [18]. Further, in order to support the presence of Ag particles, we recorded optical absorption spectra of the supernatant (collected by centrifuging the sonicated dispersion of ZAg5 sample) and it clearly shows the SPR band of Ag that confirms the presence of silver nanoparticles in the heterosystem (Supplementary material). The optical absorption spectrum of the supernatant shows Ag's SPR-related absorption band at around 413 nm and a broad absorption feature in the 600–800 nm range. Thus, the presence of nearly spherical features in the ZAg5 sample (Supplementary material) and observation of Ag-related absorption features in the optical

Fig. 3 TEM images of the silver-modified ZnO samples (ZAg3 and ZAg5). Small particles indicated with *arrow* are nearly spherical Ag nanoparticles presented along with rod-like structures of ZnO

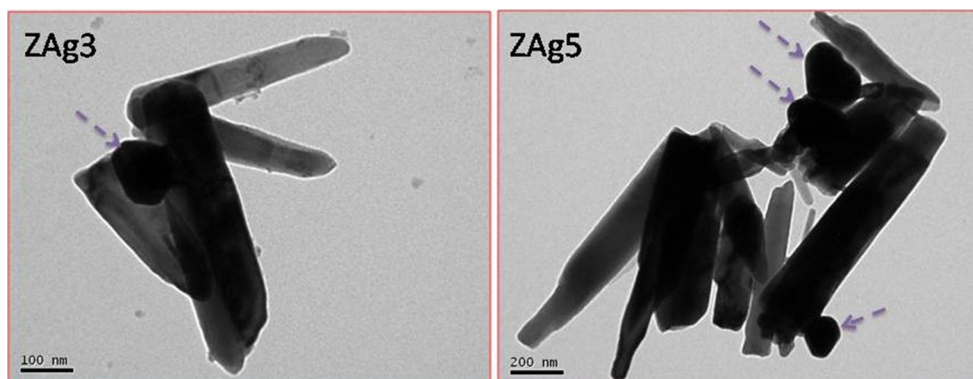
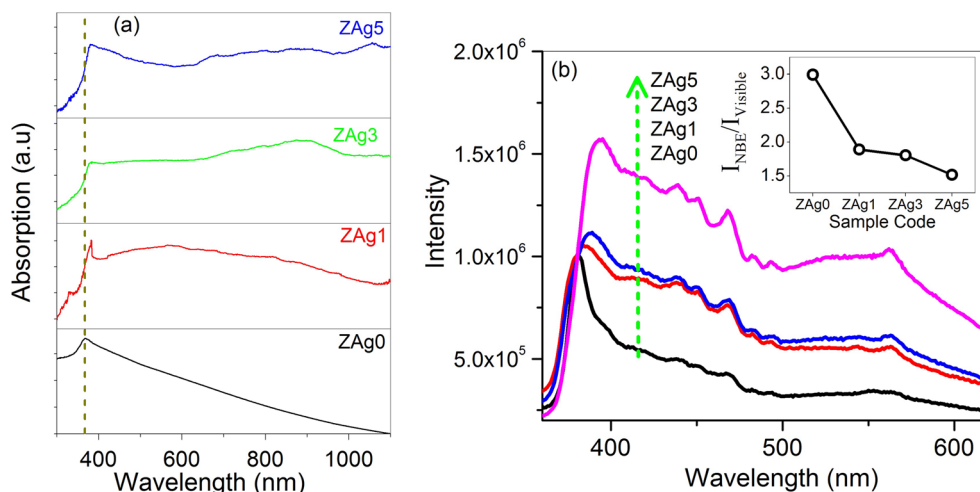


Fig. 4 **a** Optical absorption spectra of pure and silver-modified ZnO nanorods. **b** The PL spectra of unmodified and Ag-modified ZnO nanorods were measured at room temperature with an excitation wavelength of 330 nm. *Inset* of the figure depicts intensity ratio of NBE to visible emission



absorption spectra of the supernatant collected from ZAg5 sample strongly supports that prepared samples consists of Ag particles along with ZnO rods.

Photoluminescence spectra of the prepared samples are shown in Fig. 4b. Pure ZnO nanorod sample (ZAg0) showing band at around 380 nm is due to the near-band edge (NBE) emission of excitons. From Fig. 4b, it is clear that the intensity of NBE emission, which originates from the excitonic recombination in ZnO, increases with the increasing amount of the Ag [22]. This enhancement is possible by the interfacial contact present between Ag nanoparticles and ZnO nanostructures. Ag doping as an acceptor results in the availability of more holes, thereby lifting the exciton-related emission [23]. Emission related to various defect centers like zinc vacancies, interstitial zinc, oxygen vacancies, interstitial oxygen, etc. of ZnO results in broad emission which covers visible region and is observed in all the samples. Intensity of this visible emission is enhanced in the Ag-modified samples when compared with as prepared pure ZnO sample (ZAg0). Broad green emission at around 550 nm can be assigned to the presence of oxygen defects in ZnO nanorods. Inset of Fig. 4b provides the variation of intensity of NBE to visible emission (broad green emission band). Decrease in this ratio shows the increasing contribution of visible emission, which is expected as the defect centers located near the surface are influenced by the presence of metal NP's.

Tanabe [24] discussed about the dependence of the field enhancement factor on various parameters, such as wavelength, distance from the nanoparticle/nanoshell, surrounding medium, and diameter ratio between the core and the shell. The field enhancement factor calculation is based on the classical electromagnetic field theory in the quasi-static limit using empirical wavelength-dependent dielectric constants. The field enhancement factor is defined as the intensity ratio between the field around the metal nanoparticle and original incident field. When a homogeneous, isotropic sphere placed

in a medium under static electric field ($\vec{E}_0 = E_0 \hat{e}_z$), metal sphere experiences induced charge on its surface due to the difference in dielectric constants of metal sphere and medium. The field enhancement factor at a point r (observing point from the center of the sphere) is defined as [24]

$$\eta = \frac{|\vec{E}_2|^2}{|\vec{E}_0|^2} = \left| 1 + 2 \frac{a^3}{r^3} g \right|^2 \quad (1)$$

and g is defined as

$$g = \frac{\varepsilon_1 - \varepsilon_m}{\varepsilon_1 + 2\varepsilon_m} \quad (2)$$

where \vec{E}_2 is the electric field outside the sphere, a is the radius of the metal sphere, ε_1 is the dielectric constant of the metal sphere which is the function of wavelength, and ε_m is the dielectric constant of the surrounding medium, which is ZnO in our samples. Dielectric constant of the metal sphere given in the appendix of ref. [24] work based on wavelength-dependent optical constant data [25] is used in this paper. Figure 5 shows the calculated field enhancement factor η around silver nanoparticle in the medium (ZnO) for two values a/r (ratio between the radius of the metal sphere to the observing point). Surrounding medium in the present case is ZnO whose dielectric constant is size dependent. Yang et al. [26] in their work on ZnO nanowires observed a decrease of dielectric constant from 6.4 to 2.7, which is smaller than bulk ZnO value (8.66). In view of this, we calculated field enhancement factor for different dielectric constant values of the medium ($\varepsilon_m = 1, 2, 4, 6, \text{ and } 8$). These calculations make us to better understand about the influence of surrounding medium and observing point (distance from the metal nanoparticles surface) on the field enhancement factor. It is clear that the

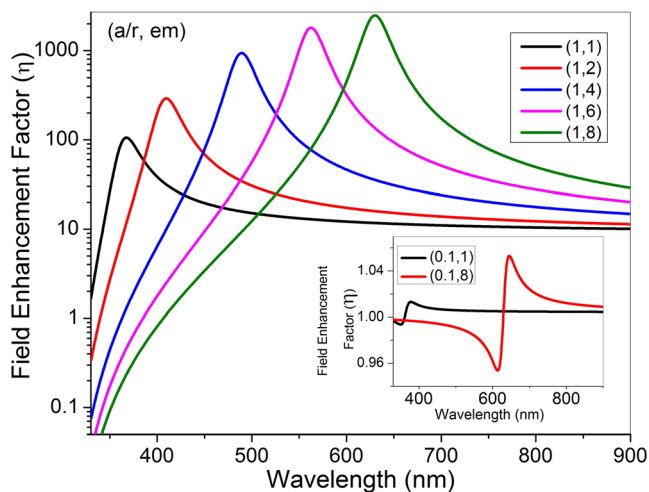


Fig. 5 Calculated field enhancement factors (η) of the Ag nanoparticle for observing point immediately adjacent to the metal particle: $(a/r)=1$. The legend of the figures is provided with $(a/r, \epsilon_m)$ values for each plot. Inset of the figure depicts η for observing point far away from the particles surface: $(a/r)=0.1$

field enhancement factor is larger when the observing point is nearer to the surface and it diminishes when the observing point moves away from the metal particles’ surface. It is observed that surrounding medium influences the peak position of the field enhancement factor, and peak position is independent of particle size. With this conceptual understanding about the nature of the concentration of electromagnetic fields around nanoparticles, we believe that the local field associated with randomly distributed metal nanoparticles, which are closely associated with ZnO nanostructures in the present system of samples under study, influences the optical and vibrational properties.

The interaction between surface plasmons of Ag and spontaneous emission of (recombination of electron-hole pairs) ZnO will also contribute to the observed enhancement of photoluminescence. Lai et al. [27] reported about large enhancement in emission intensity from ZnO films capped by Ag while negligible effect from Au-coated films and this enhancement was attributed to resonant coupling. Resonance energies of plasmons at different interfaces can be determined by considering the following dispersion relation [27]

$$hk_{sp} = E_i \sqrt{\frac{\epsilon_m \epsilon_d}{\epsilon_m + \epsilon_d}}$$

where E_i is the incident energy, ϵ_m and ϵ_d are dielectric constants of metal and dielectric medium, respectively, and k_{sp} is the wave vector of surface plasmon. Based on the above relation, Lai et al. [27] reported that ZnO, whose luminescence falls between the determined resonance energies of surface plasmon at Ag/ZnO (2.93 eV) and Ag/air interfaces (3.7 eV), has a high rate of resonant coupling with the presence of Ag

nanoparticles, and this supports our observed enhanced luminescence from ZnO after Ag modification.

Raman Spectral Analysis

Figure 6 shows the Raman scattering spectra for pure and Ag-modified ZnO nanorods recorded at room temperature using Ar ion laser source (514.5 nm). As per group theory predictions, wurtzite ZnO (having two formula units per primitive cell) belongs to the C_{6v}^4 space group. Usually Raman spectra of ZnO exhibits E_{2Low} , E_{2High} , longitudinal optical (LO), transverse optical (TO) phonon modes as Raman active modes and modes related to second order process (like $2E_{2Low}$, $E_{2High} - E_{2Low}$, etc.) will also be observed. Apart from these, phonon modes related to silent modes (B_{1Low} , $2 B_{1Low}$) and local lattice vibration or disorder-induced scattering-related modes will also be observed [28].

From Fig. 6, Raman spectra of pure ZnO (ZAg0) shows prominent peaks at ~ 100 and $\sim 438 \text{ cm}^{-1}$ that corresponds to the Raman process related to E_{2Low} and E_{2High} phonon modes which are associated with the vibration of Zn and O atoms in the ZnO lattice, respectively. Weak bands appeared at ~ 335 , ~ 381 and $\sim 578 \text{ cm}^{-1}$ which corresponds to $E_{2High} - E_{2Low}$, $A_1(TO)$, and quasi-*LO* phonon modes, respectively. These Raman bands does not show any remarkable shift in their position in the Ag-modified ZnO samples [29, 30]. The extra prominent band around $\sim 225 \text{ cm}^{-1}$ observed in the Ag-modified samples is attributed to the mode that arises from Ag and chemisorbed molecular oxygen species on the Ag [29].

Raman modes appeared at around ~ 1379 and $\sim 1585 \text{ cm}^{-1}$ are observed in the Ag-modified samples alone. The former band can be assigned to the mode arise from vibration related to Ag and interstitial oxygen and later mode can be assigned to structural defects that arises due to Ag presence while these two modes are not shown by pure ZnO [31, 32]. Perhaps these

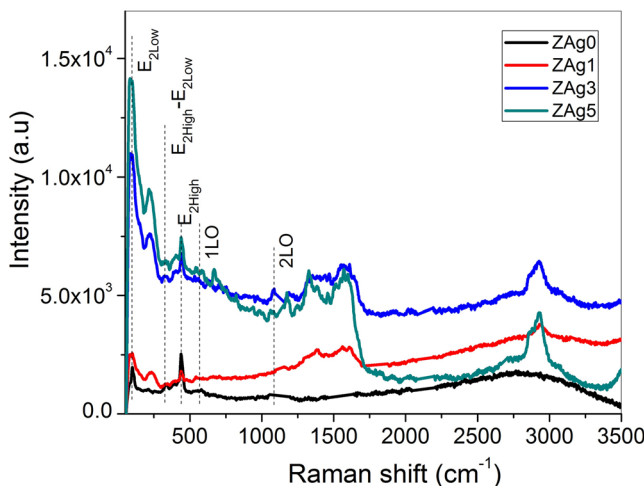


Fig. 6 Raman spectra for the pure and Ag-modified ZnO nanorod samples excited with Ar ion laser source

modes fall in the range of the well-known D and G bands of the disordered graphitic carbon [33]. At this stage, its highly difficult to comment on the origin of these modes as the presence of carbon on the surface and enhancement of the Raman signal of the surface adsorbents due to metallic silver, by local field enhancement, cannot be ruled out in the case of our samples. Higher order Raman modes of the Ag-modified ZnO samples in the range of 2500–3500 cm^{-1} are visible with good resolution when compared with the pure ZnO Raman spectrum [21, 32, 33].

Compared to pure ZnO, Ag-modified ZnO nanorod sample shows enhanced Raman scattering, and this enhancement arises due to the local field associated with metal nanoparticles at the interfaces of ZnO and Ag. Metal nanoparticle induced local field scaled up the active phonon interactions and also enhanced the scattering associated with higher order phonon modes [34, 35]. Observation of intensity enhancement with the presence of Ag nanoparticles resembles SERS-like behavior of ZnO sample with randomly distributed metallic Ag nanoparticles. Two enhancement mechanisms: electromagnetic and chemical enhancements contribute to the surface-enhanced Raman scattering (SERS). The local field enhancement in the surroundings of metal nanoparticles is the origin for the former enhancement mechanism and later originates from the electron transfer between the semiconductor and metal nanoparticles [36].

Rumyantseva et al. [37] reported pronounced enhancement of Raman scattering from ZnO nanocrystals on substrates coated with Ag nanoparticles and possible explanation as a theory to understand this enhancement is given, which contains three contributing factors for the Raman scattering enhancement factor, F_{RS} . Raman scattering enhancement factor, F_{RS} in the vicinity of metal nanoparticle for a probe located at a point r is given by [37]

$$F_{\text{RS}}(\omega, \omega', r) = G_I(\omega, r) G_{\text{LDOS}}(\omega', r) G(\omega, r)$$

where $G(\omega, r)$ is Gersten-Nitzan factor (contribution of field reflected from a nanobody), $G_I(\omega, r) = I(\omega, r)/I_o(\omega)$ is the incident field enhancement factor (for light intensity I_o and frequency ω) and $G_{\text{LDOS}}(\omega', r)$ is enhancement factor related to the local photon density of states with respect to vacuum density of states. This enhancement factor is metal nanoparticle size dependent. As discussed earlier in the section of this manuscript, when the wavelength of the incident light is close to the surface plasmon wavelength of the metal nanoparticles, large electromagnetic field surrounding the surface of these metal nanoparticles makes the way for enhanced Raman scattering of ZnO system.

Conclusion

In summary, cost-effective synthesis route is chosen for the successful preparation of pure and Ag-modified ZnO nanostructures. From the XRD patterns, Ag doping-induced lower angle shift is observed. The presence of metallic silver is identified from the extra XRD peaks related to metallic silver. Optical absorption studies show a decrease of band gap for Ag-modified ZnO when compared with pure ZnO sample. Broad optical absorption in the visible region is attributed to the SPR absorption of Ag nanoparticles, whose presence along with ZnO is supported by the XRD studies. From this work, we attempted to understand the observed enhancement in photoluminescence and Raman scattering in the view of the local field associated with the metal nanoparticles. The observed enhancement in luminescence and high Raman signals with lower laser intensities in case of Ag-modified ZnO nanorod samples makes these materials as a promising candidate for bio-imaging/bio-labeling applications where one can take advantage of ZnO nanostructures with enhanced luminescence and Raman scattering.

References

- Aslan K, Wu M, Lakowicz JR, Geddes CD (2007) Fluorescent core-shell Ag@SiO₂ nanocomposites for metal-enhanced fluorescence and single nanoparticle sensing platforms. *J Am Chem Soc* 129:1524
- Liu L, Miao P, Xu Y, Tian Z, Zou Z, Li G (2010) Study of Pt/TiO₂ nanocomposite for cancer-cell treatment. *J Photochem Photobiol B* 98:207
- Wei Y, Li Y, Liu X, Xian Y, Shi G, Jin L (2010) ZnO nanorods/Au hybrid nanocomposites for glucose biosensor. *Biosens Bioelectron* 26:275
- Shan G, Wang S, Fei X, Liu Y, Yang G (2009) Heterostructured ZnO/Au nanoparticles-based resonant Raman scattering for protein detection. *J Phys Chem B* 113:1468
- Aldeek F, Mustin C, Balan L, Medjahdi G, Carmes TR, Arnoux P, Schneider R (2011) Enhanced photostability from CdSe(S)/ZnO core/shell quantum dots and their use in biolabeling. *Eur J Inorg Chem* 2011:794
- Asifa MH, Usman Ali SM, Nur O, Willander M, Englund UH, Elinder F (2010) Functionalized ZnO nanorod-based selective magnesium ion sensor for intracellular measurements. *Biosens Bioelectron* 26:1118
- Wu YL, Lim CS, Fu S, Tok AIY, Lau HM, Boey FYC, Zeng XT (2007) Surface modifications of ZnO quantum dots for bio-imaging. *Nanotechnology* 18:215604
- Stuart HR, Hall DG (1996) Absorption enhancement in silicon-on-insulator waveguides using metal island films. *Appl Phys Lett* 69:16
- Deng S, Fan HM, Zhang X, Loh KP, Cheng CL, Sow CH, Foo YL (2009) An effective surface-enhanced Raman scattering template based on a Ag nanocluster–ZnO nanowire array. *Nanotechnology* 20:175705
- Aslan K, Leonenko Z, Lakowicz JR, Geddes CD (2005) Annealed silver-island films for applications in metal-enhanced fluorescence: interpretation in terms of radiating plasmons. *J Fluoresc* 15:643

11. Tang H, Meng G, Huang Q, Zhang Z, Huang Z, Zhu C (2012) Arrays of cone-shaped ZnO nanorods decorated with Ag nanoparticles as 3D surface-enhanced Raman scattering substrates for rapid detection of trace polychlorinated biphenyls. *Adv Funct Mater* 22:218
12. Lee J, Govorov AO, Dulka J, Kotov NA (2004) Bioconjugates of CdTe nanowires and Au nanoparticles: plasmon-exciton interactions, luminescence enhancement, and collective effects. *Nano Lett* 4:2323
13. Ansari SA, Khan MM, Ansari MO, Lee J, Cho MH (2013) Biogenic synthesis, photocatalytic, and photoelectrochemical performance of Ag-ZnO nanocomposite. *J Phys Chem C* 117:27023
14. Zhang WQ, Lu Y, Zhang TK, Xu W, Zhang M, Yu SH (2008) Controlled synthesis and biocompatibility of water-soluble ZnO nanorods/Au nanocomposites with tunable UV and visible emission intensity. *J Phys Chem C* 112:19872
15. Guo SH, Heetderks JJ, Kan HC, Phaneuf RJ (2008) Enhanced fluorescence and near-field intensity for Ag nanowire/nanocolumn arrays: evidence for the role of surface plasmon standing waves. *Opt Express* 16:18417
16. Lupan O, Chow L, Ono LK, Cuenya BR, Chai G, Khallaf H, Park S, Schulte A (2010) Synthesis and characterization of Ag- or Sb-doped ZnO nanorods by a facile hydrothermal route. *J Phys Chem C* 114:12401
17. Georgekutty R, Seery MK, Pillai SC (2008) A highly efficient Ag-ZnO photocatalyst: synthesis, properties, and mechanism. *J Phys Chem C* 112:13563
18. Liu HR, Shao GX, Zhao JF, Zhang ZX, Zhang Y, Liang J, Liu XG, Jia HS, Xu BS (2012) Worm-like Ag/ZnO core-shell heterostructural composites: fabrication, characterization, and photocatalysis. *J Phys Chem C* 116:16182
19. Wang YS, Thomas PJ, O'Brien P (2006) Optical properties Of ZnO nanocrystals doped with Cd, Mg, Mn, and Fe ions. *J Phys Chem B* 110:21412
20. Irimpan L, Nampoori VPN, Radhakrishnan P (2010) Spectral and nonlinear optical characteristics of ZnO nanocomposites. *Sci Adv Mater* 2:117
21. Li F, Liu X, Qin Q, Wu J, Li Z, Huang X (2009) Sonochemical synthesis and characterization of ZnO nanorod/Ag nanoparticle composites. *Cryst Res Technol* 44:1249
22. Irimpan L, Nampoori VPN, Radhakrishnan P (2006) Spectral and nonlinear optical characteristics of nanocomposites of ZnO–Ag. *Chem Phys Lett* 455:265
23. Duan L, Lin B, Zhang W, Zhong S, Fua Z (2006) Enhancement of ultraviolet emissions from ZnO films by Ag doping. *Appl Phys Lett* 88:232110
24. Tanabe K (2008) Field enhancement around metal nanoparticles and nanoshells: a systematic investigation. *J Phys Chem C* 112:15721
25. Palik ED (1985) Handbook of optical constants of solids. Academic, New York
26. Yang Y, Guo W, Wang X, Wang Z, Qi J, Zhang Y (2012) Size dependence of dielectric constant in a single pencil-like ZnO nanowire. *Nano Lett* 12:1919
27. Lai CW, An J, Ong HC (2005) Surface-plasmon-mediated emission from metal-capped ZnO thin films. *Appl Phys Lett* 86:251105
28. Cuscó R, Lladó EA, Ibáñez J, Artús L (2007) Temperature dependence of Raman scattering in ZnO. *Phys Rev B* 75:165202
29. Xie W, Li Y, Sun W, Huang J, Xie H, Zhao X (2010) Surface modification of ZnO with Ag improves its photocatalytic efficiency and photostability. *J Photochem Photobiol A* 216:149
30. Ren C, Yang B, Wu M, Xu J, Fu Z, lv Y, Guo T, Zhao Y, Zhu C (2010) Synthesis of Ag/ZnO nanorods array with enhanced photocatalytic performance. *J Hazard Mater* 182:123
31. Gangopadhyay P, Kesavamoorthy R, Nair KGM, Dhandapani R (2000) Raman scattering studies on silver nanoclusters in a silica matrix formed by ion-beam mixing. *J Appl Phys* 88:4975
32. Hadad L, Perkas N, Gofer Y, Moreno JC, Ghule A, Gedanken A (2007) Sonochemical deposition of silver nanoparticles on wool fibers. *J Appl Polym Sci* 104:1732
33. Bhattacharyya S, Gedanken A (2008) Microwave-assisted insertion of silver nanoparticles into 3-D mesoporous zinc oxide nanocomposites and nanorods. *J Phys Chem C* 112:659
34. Messinger BJ, Raben KU, Chang RK, Barber PW (1981) Local fields at the surface of noble-metal microspheres. *Phys Rev B* 2:649
35. Zhu J (2007) Spatial dependence of the local field enhancement in dielectric shell coated silver nanospheres. *Appl Surf Sci* 253:8729
36. Liu CY, Dvoynenko MM, Lai MY, Chan TH, Lee YR, Wang JK, Wang YL (2010) Anomalously enhanced Raman scattering from longitudinal optical phonons on Ag-nanoparticle-covered GaN and ZnO. *Appl Phys Lett* 96:033109
37. Romyantseva A, Kostcheev S, Adam PM, Gaponenko SV, Vaschenko SV, Kulakovich OS, Ramanenka AA, Guzatov DV, Korbutyak D, Dzhagan V, Stroyuk AL, Shvalagi VV (2013) Non-resonant surface enhanced Raman scattering of ZnO quantum dots with Au and Ag nanoparticles. *ACS Nano* 7:3420